Proceedings of The Third International Symposium

TEXTILE COMPOSITES IN BUILDING CONSTRUCTION

November 7-9, 1996, Seoul, Korea
Sheraton Walker Hill Hotel

Cosponsored by
THE KOREAN SOCIETY FOR COMPOSITE MATERIALS
&
THE KOREAN FIBER SOCIETY

Proceedings of The Third International Symposium

TEXTILE COMPOSITES IN BUILDING CONSTRUCTION

T C I B C

November 7-9, 1996, Seoul, Korea
Sheraton Walker Hill Hotel

Cosponsored by
THE KOREAN SOCIETY FOR COMPOSITE MATERIALS
&
THE KOREAN FIBER SOCIETY

	S3(A) Camellia Room	S4(A) Rose Room
	Chair : K. S. Han and R. Houtman	Chair : H.J. Choo and J. Karger-Kocsis
15:20	**The Experimental Study on the Effect of Reinforcing the Rectangular Beam Shearing due to Carbon Fiber Sheet.** H. Sakai*, H. Otaguro*, N. Hisabe*, Y. Mitsui**,K.Murakami** (*Mitsubishi Chemical Co, **Kumamoto Univ., Japan)	**Enhanced Properties of Epoxy Resins with Phosphorus Containing Ploymers.** I. Y. Park*, I. C. Kim*, Y. R. Park*, Y. D. Choi*, T. H. Yoon*, J. I. Yuck**, S. G. Lee** (*K-JIST,**Agency for Defense Development, Korea)
15:45	**Experimental Study of Stiffened Composite Plates Loaded in Axial Compression.** C.-S. Hong, C.-G. Kim, C.-W. Kong, I.-C. Lee (KAIST, Korea)	**Active Vibration Control of Composite Structures with Piezo-ceramic Actuator and Piezo-film Sensor.** J.-H. Han, I. Lee (KAIST, Korea)
16:10	**The Effect of Neglecting Own Weight on the Natural Frequency of Vibration of Laminated Composite Plates with Attached Mass/Masses.** D.-H. Kim (Korea Composites, Korea)	**Study on the House Wrapping Performa nce of Nonwoven Composites.** H.-Y. Jeon (Chonnam National Univ., Korea)
16:35	**Thermal Stresses in the Vicinity of the Through-thickness Stitch in a Cylindrical Cross-Ply Laminate.** M. W. Hyer*, H. H. Lee** (*Virginia Polytechnic Institute & State Univ., U.S.A. **Korea Aerospace Research Institute, Korea)	**Study on the Development of Compo site Artificial Leg Shell.** B.-S. Kim, M.-K. Um (Korea Institute of Machinery & Materials, Korea)
17:00	**The influence of Distortion Introduced by Cloth Flattening on Stress Behaviour of Tensile Structures.** R. Houtman*, L. Grundig** (*Delft Univ. of Technology, Netherlands, **Berlin Univ. of Technology, Germany)	**Fracture and Failure Behavior of Glass Fiber Mat-Reinforced Thermoplastics (GMT-PP)** J. Karger-Kocsis, M. Neitzel (Univ. of Kaiserslautern, Germany)
17:25	**Analytical Model for Thermal Expansion Coefficients of plain Woven Fabric Composites.** S.-K. Lee*, S.-H. Hong**, J.-H. Byun* (*Korea Institute of Machinery & Materials, **KAIST, Korea)	**Development of Process for Making Para Aramid Pulp without Spinning Process.** M. S. Rhim (KOLON Ind. Inc, Korea)
17:50	**A Simple Method for Calculating the Natural Frequencies of Simple Supported Composite Plates with Non-uniform Cross-section and with Attached Masses.** D.-H. Kim (Korea Composites, Korea)	**Mechanical ProPerties of Nonworen Glass Fiber Composite.** S. H. Lee, T. J. Kang (Seoul National Univ., Korea)

for reducing the structural noise and vibration. Among several methods to suppress structural vibration, the use of piezoelectric materials has been drawn attention. They can be easily incorporated into conventional structures, and they can be easily manufactured into the desired shapes. Bailey and Hubbard Jr. [1] investigated the use of surface-bonded piezo film actuators to reduce vibrations in a cantilevered beam. Choi [2] performed vibration reduction experiment for a cantilevered beam using multi-step bang bang control methods. Tzou and Gadre [3] demonstrated vibration reduction of a beam using variable feedback gains. Lazarus and Crawley [4] used LQG (Linear Quadratic Gaussian) control and Optimal projection compensation to control vibration of a plate specimen.

There have been researches to analyze the structures with piezoelectric materials. Lee [5] introduced a consistent plate model based on classical laminated plate theory. Hwang et al. [6] developed a finite element formulation for piezo-laminated plates. There have been a lot of studies to utilize piezoelectric materials for vibration reduction of isotropic structures. However, there should be more studies for vibration reduction of composite structures. In this study a finite element formulation for piezo-laminated plate has been developed and experimental tests for vibration control of composite beams and plates have been performed.

Finite Element Formulation

In this section a brief description of the finite element procedures for piezo-laminated composite plates is presented. The modeling procedures are similar to that of Lee [5], and finite element procedures are based on the Reddy's work [7]. In this study the first-order shear deformation theory (FSDT) is used to analyze the piezo-laminated composite plate, because it is well known that the inclusion of shear deformation gives quite accurate results for composite plates. Another reason for that is simplicity in formulating a finite element model because this theory requires only C^0 element.

The linear constitutive equations of a lamina can be given as follows:

$$\{\hat{\sigma}\} = [Q]\{\hat{\varepsilon}\} - [e]^T\{E\} \quad (1)$$

$$\{D\} = [e]\{\hat{\varepsilon}\} + [\varepsilon]\{E\} \quad (2)$$

where $\{\hat{\sigma}\}$ is the stress, $\{\hat{\varepsilon}\}$ is the strain, $\{E\}$ is the electric field, $\{D\}$ is the electric displacement, $[Q]$ is the elastic stiffness matrix, $[e]$ is the piezoelectric stress coefficient, and $[\varepsilon]$ is the permittivity matrix. In Equations (1) and (2) a lamina can be either a piezoelectric material or a conventional composite lamina. In the latter case material constants $[e]$ and $[\varepsilon]$

should be set to zero. After some manipulation such as coordinate transformation, resultant forces and moments can be written as

$$\begin{Bmatrix} \mathbf{N} \\ \mathbf{M} \end{Bmatrix} = \begin{bmatrix} \mathbf{A} & \mathbf{B} \\ \mathbf{B} & \mathbf{D} \end{bmatrix} \begin{Bmatrix} \boldsymbol{\varepsilon}^0 \\ \boldsymbol{\kappa}^0 \end{Bmatrix} - \begin{Bmatrix} \mathbf{N}^C \\ \mathbf{M}^C \end{Bmatrix}, \quad \begin{Bmatrix} Q_y \\ Q_x \end{Bmatrix} = \begin{bmatrix} \overline{A}_{44} & \overline{A}_{45} \\ \overline{A}_{45} & \overline{A}_{55} \end{bmatrix} \begin{Bmatrix} \varepsilon_{yz}^0 \\ \varepsilon_{xz}^0 \end{Bmatrix} \tag{3}$$

where $\mathbf{N}$ and $\mathbf{M}$ are force and moment resultants of the plate, respectively; $\mathbf{N}^C$ and $\mathbf{M}^C$ are piezoelectric actuation force and moment resultants; Q_y and Q_x are shear force resultants; $\boldsymbol{\varepsilon}^0$ and $\boldsymbol{\kappa}^0$ are midplane strains and curvature; and ε_{yz}^0 and ε_{xz}^0 are shear strains. $\mathbf{A}$, $\mathbf{B}$ and $\mathbf{D}$ are the respective inplane, bending-stretching and the bending stiffnesses of the plate, respectively, and $\overline{A}_{ij}$ (i, j = 4, 5) denote the shear stiffness coefficients.

The displacement field in the shear deformation theory can be written as follows:

$$\begin{aligned} u(x,y,z,t) &= u_0(x,y,t) + z\phi_x(x,y,t) \\ v(x,y,z,t) &= v_0(x,y,t) + z\phi_y(x,y,t) \\ w(x,y,z,t) &= w_0(x,y,t) \end{aligned} \tag{4}$$

where t is the time, u, v and w are the displacements in the x, y and z directions, respectively; u_0, v_0 and w_0 are the associated midplane displacements; and ϕ_x and ϕ_y are the rotations in the xz and yz planes. After discretization of the domain, displacements can be interpolated by the form of Equation (5).

$$(u_0, v_0, w_0, \phi_x, \phi_y) = \sum_{i=1}^{m} (u_{0i}, v_{0i}, w_{0i}, \phi_{x_i}, \phi_{y_i}) \hat{\psi}_i \tag{5}$$

Variational principle for the plate can be written as

$$\begin{aligned} \int_0^T \int_\Omega [& N_x \frac{\partial \delta u_0}{\partial x} + M_x \frac{\partial \delta \phi_x}{\partial x} + N_y \frac{\partial \delta v_0}{\partial y} + M_y \frac{\partial \delta \phi_y}{\partial y} + N_{xy}\left(\frac{\partial \delta u_0}{\partial y} + \frac{\partial \delta v_0}{\partial x}\right) \\ & + M_{xy}\left(\frac{\partial \delta \phi_x}{\partial y} + \frac{\partial \delta \phi_y}{\partial x}\right) + Q_y\left(\delta \phi_y + \frac{\partial \delta w_0}{\partial y}\right) + Q_x\left(\delta \phi_x + \frac{\partial \delta w_0}{\partial x}\right) \\ & + I_1(\ddot{u}_0 \delta u_0 + \ddot{v}_0 \delta v_0 + \ddot{w}_0 \delta w_0) + I_3(\ddot{\phi}_x \delta \phi_x + \ddot{\phi}_y \delta \phi_y) \\ & + I_2(\ddot{u}_0 \delta \phi_x + \ddot{\phi}_x \delta u_0 + \ddot{v}_0 \delta \phi_y + \ddot{\phi}_y \delta v_0) - q \delta w_0] dA\, dt = 0 \end{aligned} \tag{6}$$

where $\ddot{(\,)} = d^2(\,)/dt^2$, $(I_1, I_2, I_3) = \int_{-h/2}^{h/2} (1, z, z^2) \rho dz$, and ρ is the mass density. With the use of Equations (5) and (6), the finite element equations can be obtained as follows:

$$[\mathbf{M}]\{\ddot{\Delta}\} + [\mathbf{K}]\{\Delta\} = \{\mathbf{F}^{ext}\} + \{\mathbf{F}\} \tag{7}$$

where $[\mathbf{M}]$, $[\mathbf{K}]$, and $\{\Delta\}$ are mass matrix, stiffness matrix, and nodal displacement vector of the whole system, respectively. $\{\mathbf{F}^{ext}\}$ is the external force vector and $\{\mathbf{F}\}$ is the piezo-actuation force vector. $\{\mathbf{F}\}$ can be written as a linear combination of $\{\overline{\mathbf{F}}\}_i$.

$$\{\mathbf{F}\} = \{\overline{\mathbf{F}}\}_1 V_1 + \{\overline{\mathbf{F}}\}_2 V_2 + \cdots + \{\overline{\mathbf{F}}\}_M V_M \tag{8}$$

where $\{\overline{\mathbf{F}}\}_j$ is the induced force vector due to unit voltage applied at the j-th actuator, V_j is the applied voltage of the j-th actuator, and M is the number of actuators. Similar derivation can be made to obtain sensor equation, and the resulting equation can be written as follows:

$$q_j = \{\overline{\mathbf{q}}\}_j^T \{\Delta\} \quad \text{or} \quad i_j = \{\bar{i}\}_j^T \{\dot{\Delta}\} \tag{9}$$

where the i-th component of $\{\overline{\mathbf{q}}\}_j$ vector is the induced charge of sensor j due to the i-th unit nodal displacement and the i-th component of $\{\bar{i}\}_j$ vector is the induced current of sensor j due to the i-th unit nodal velocity. In this analysis nine-node quadrilateral isoparametric elements are used, and reduced integration is performed in order to avoid shear locking.

Controller Design

Generally the equation of motion for flexible structures can be written as the following form.

$$\mathbf{M}\ddot{\mathbf{z}} + \mathbf{C}\dot{\mathbf{z}} + \mathbf{K}\mathbf{z} = \mathbf{F} \tag{10}$$

After transformation of eq. (10) into state space form, eq. (11) can be obtained.

$$\ddot{\eta}_i + 2\varsigma_i \omega_i \dot{\eta}_i + \omega_i^2 \eta_i = b_i \mathbf{u} \tag{11}$$

When state variable $\mathbf{x}$ is defined as modal displacements and modal velocity, the state space modal equation for the system can be written as follows:

$$\dot{\mathbf{x}} = \mathbf{A}\mathbf{x} + \mathbf{B}\mathbf{u} \tag{12}$$
$$\mathbf{y} = \mathbf{C}\mathbf{x} \tag{13}$$

where

$$\mathbf{x} = \begin{Bmatrix} \mathbf{x}_1 \\ \mathbf{x}_2 \\ \vdots \end{Bmatrix}, \quad \mathbf{A} = diag.(\mathbf{A}_i), \quad \mathbf{B} = \begin{bmatrix} \mathbf{B}_1 \\ \mathbf{B}_2 \\ \vdots \end{bmatrix}, \quad \mathbf{C} = \begin{bmatrix} \mathbf{C}_1 & \mathbf{C}_2 & \cdots \end{bmatrix} \tag{14}$$

where

$$\mathbf{A}_i = \begin{bmatrix} 0 & 1 \\ -\omega_i^2 & -2\varsigma_i\omega_i \end{bmatrix}, \quad \mathbf{B}_i = \begin{bmatrix} 0 \\ \mathbf{b}_i \end{bmatrix}$$

$$\mathbf{C}_i = \begin{bmatrix} \mathbf{c}_i & 0 \end{bmatrix} \tag{15}$$

Generally optimal control methods are state feedback control, while most classical control methods are based on output feedback. Therefore to implement control system, One should prepare an algorithm which can estimate the state value from measured output. This kind of algorithm is called an observer. Among several proposed observer, Kalman filter is selected in this study, and is an optimal state observer for the system contaminated with process and measurement noise. The state space equation for system with external noise can be written as follows:

$$\dot{\mathbf{x}} = \mathbf{Ax} + \mathbf{Bu} + \mathbf{Fv} \tag{16}$$

$$\mathbf{y} = \mathbf{Cx} + \mathbf{w} \tag{17}$$

where $\mathbf{F}$ is process noise influence matrix and $\mathbf{v}$ and $\mathbf{w}$ mean process noise and measurement noise respectively. The Kalman filter dynamics can be written as eq. (18).

$$\dot{\hat{\mathbf{x}}} = \mathbf{A}\hat{\mathbf{x}} + \mathbf{Bu} + \hat{\mathbf{K}}(\mathbf{y} - \mathbf{C}\hat{\mathbf{x}}) \tag{18}$$

where $\hat{\mathbf{x}}$ is an estimated state and $\hat{\mathbf{K}}$ is Kalman filter gain. In order to obtain filter gain, the algebraic Riccati equation (19) should be solved. From eq. (19) $\hat{\mathbf{P}}$ is obtained, and then filter gain $\hat{\mathbf{K}}$ is written as eq. (20).

$$0 = \mathbf{A}\hat{\mathbf{P}} + \hat{\mathbf{P}}\mathbf{A}^{\mathrm{T}} - \hat{\mathbf{P}}\mathbf{C}^{\mathrm{T}}\mathbf{W}^{-1}\mathbf{C}\hat{\mathbf{P}} + \mathbf{FVF}^{\mathrm{T}} \tag{19}$$

$$\hat{\mathbf{K}} = \hat{\mathbf{P}}\mathbf{C}^{\mathrm{T}}\mathbf{W}^{-1} \tag{20}$$

The objective function J for vibration reduction can be formulated in a quadratic form as eq. (21). Then control voltage can be obtained as eq. (22).

$$J = E\{\lim_{T \to \infty} \frac{1}{T} \int_0^T (\mathbf{x}^{\mathrm{T}}\mathbf{Qx} + \mathbf{u}^{\mathrm{T}}\mathbf{Ru})\,dt\} \tag{21}$$

$$\mathbf{u} = -\mathbf{G}\hat{\mathbf{x}} \tag{22}$$

where $\mathbf{Q}$ is a state weight matrix, $\mathbf{R}$ is a control weight matrix, and $\mathbf{G}$ is control gain. For more rapid vibration reduction larger value for $\mathbf{Q}$ can be selected, and for less energy consumption larger value for $\mathbf{R}$ can be selected. The process for determining control gain $\mathbf{G}$ is similar to that for filter gain, and can be summarized as follows.

$$\mathbf{KA} + \mathbf{A}^{\mathrm{T}}\mathbf{K} + \mathbf{Q} - \mathbf{KBR}^{-1}\mathbf{B}^{\mathrm{T}}\mathbf{K} = \mathbf{0} \tag{23}$$

$$\mathbf{G} = \mathbf{R}^{-1}\mathbf{B}^{\mathrm{T}}\mathbf{K} \tag{24}$$

As discussed so far, a control procedure which uses Kalman filter as an observer and a controller that minimizes an objective function of quadratic form is called LQG (Linear Quadratic Gaussian) control method.

Constant gain control method and bang-bang control method, which belong to classical control, are based on the measured output instead of estimated state. Therefore their structures are relatively simple and the control input can be written as follows:

$$\text{CGC:}\quad F = -K_d \cdot \left(\frac{dy}{dt}\right) \qquad \text{BBC:}\quad F = -V_{\max} \cdot \operatorname{sgn}\left(\frac{dy}{dt}\right) \tag{25}$$

Experiments and Results

The composite structures used in vibration control have been manufactured at an autoclave in the Dept. of Aerospace Eng., KAIST. The Graphite/epoxy prepreg is used, and beam and plate type specimens were made using a diamond cutter. Piezo-film sensor and piezo ceramic actuator were bonded to the proper location of composite structures. The dimensions and configurations are demonstrated in Figs. 1 and 2. For beam specimen (stacking sequence : $[90_2/0]_S$) a piezo ceramic was bonded near the clamped boundary in order to produce efficient moment. The material properties for composite lamina and piezo materials are given in Table 1. As seen in eq. (15), natural frequencies and modal damping ratio should be identified. In addition, modal actuation forces and modal sensing constants should be identified. Natural frequencies are measured from the frequency response function between the random signal applied to piezo ceramic and measured output signal from piezo film. Modal damping ratios are obtained from the envelope of the damped free vibration signal. Modal actuation forces and modal sensor constants are obtained from steady state excitation experiment.

The overall experimental setup for vibration control is shown in Fig. 3. The external disturbances make the composite structure vibrate, and a piezo film sensor generates charge.

Table 1 Material Properties of Composite Lamina (HFG Gr/Epoxy), Piezoceramics (Fuji C-82) and Piezofilm (PFS LDT2-028K).

	HFG Gr/Epoxy	Fuji C-82	PFS LDT2-028K
E_1 (GPa)	130	59	—
E_2(GPa)	10.0	59	—
G_{12}(GPa)	4.85	22	—
G_{23}(GPa)	3.29	21	—
υ_{12}	0.31	0.34	—
ρ(kg/m^3)	1480	7400	1780
d_{31}(pC/N)	—	-260	23
d_{32}(pC/N)	—	-260	—
g_{31}(x10^{-3}m^2/C)	—	-8.7	216
g_{32}(x10^{-3}m^2/C)	—	18.0	-339

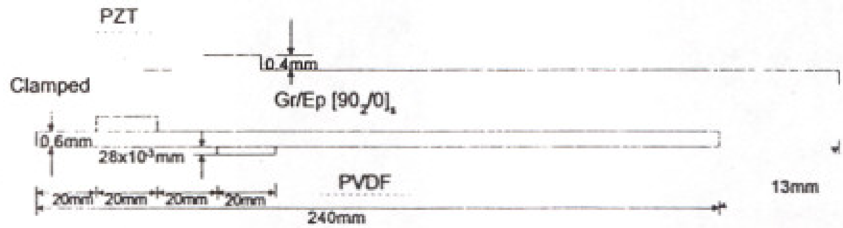

Fig. 1 Composite beam with piezo sensor and actuator.

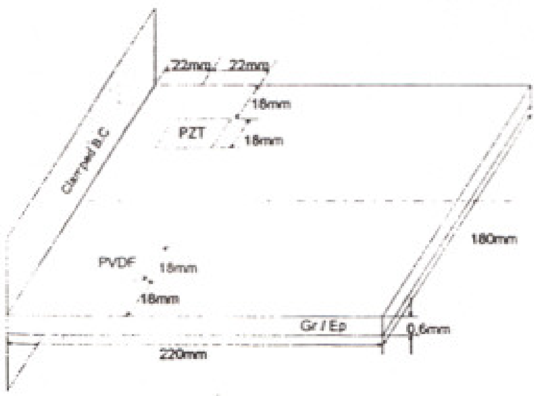

Fig. 2 Composite plate with piezo sensor and actuator.

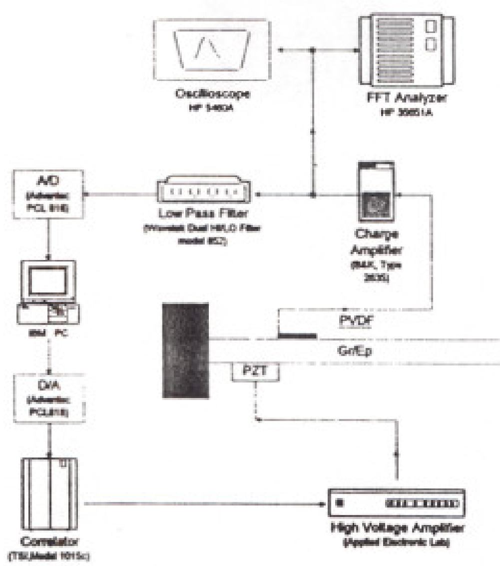

Fig. 3 Overall experimental setup.

The charge is transformed into voltage through charge amplifier(B&K Type 2635). In order to reduce the effects of high frequency noise, a low pass filter (Waveteck Dual HI/LO Filter model 852) is used. The signal is fed into PC(personal computer) via analog-digital conversion card(Advantec PCL 818), and PC performs the required calculations to make control signal. That is, Kalman filter and LQ optimal controller are implemented in a PC. The implementation of several control algorithm can be done easily using this kind of controller. The control signal is processed in a correlator (TSI Model 1015C) to remove DC offset, and amplified in a high voltage amplifier (Applied Electronics Lab.). The maximum voltage is limited to 150 V for this high voltage amplifier. A digital oscilloscope and a FFT analyzer are used to monitor the vibration reduction effects.

To quantify the relative importance of weighting matrix Q and R, the following numerical value is adopted in the beam vibration control experiment.

$$\mathrm{R} = 1/m, \quad \mathrm{Q} = diag.(9\times10^{7}, 4.04\times10^{9}, 6.0\times10^{5}, 1.23\times10^{8}) \qquad (26)$$

The representative results for the fist mode vibration are plotted in Fig. 4. The simulation results obtained from finite element method and MATLAB/SIMULINK are plotted in Fig. 5. From Figs. 4 and 5 it is found that the developed finite element model predicts the dynamic and control behavior of the beam specimen to fairly good degrees. For the sake of brevity other control results are not shown here, but it is also found that as the value of m increases the control effects become larger. It was also observed that LQG control has more advantages than classical control when simultaneous control of two vibrational modes is performed. In Fig. 6 the frequency response of the beam is plotted. The LQ control makes the first frequency increase, and reduce the peak value of the first two modes. It seems that there is a little effect of closed loop control on the third mode. To evaluate the performance of present experimental methods further, composite plate specimens were manufactured and tested. Two kinds of plates were prepared. They are identical except for the stacking sequence. The stacking sequence of plate 3 is $[\pm 60/0]_S$, and that of plate 4 is $[90/0_2]_S$. Plate 1 and 2 were used in a preliminary test. Simultaneous control results of the first two modes are shown in Fig. 7 and 8. For plate 3, the first and second resonance peak were reduced around 10dB. In the case of plate 4 the third frequency and the fourth frequency are close, and so called spillover effects are large. So it is hard to increase damping of the first and second mode further. However it should be noted that it is very hard to control more than one modes simultaneously using classical control methods.

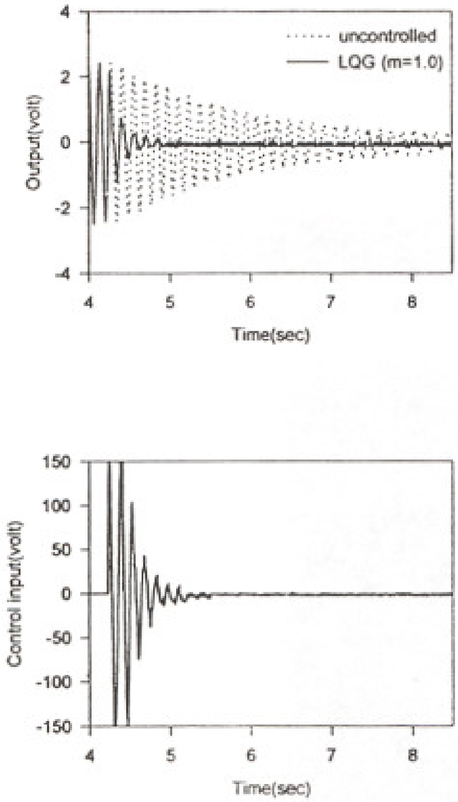

Fig. 4 Experimental results of LQ control for the first mode of beam.

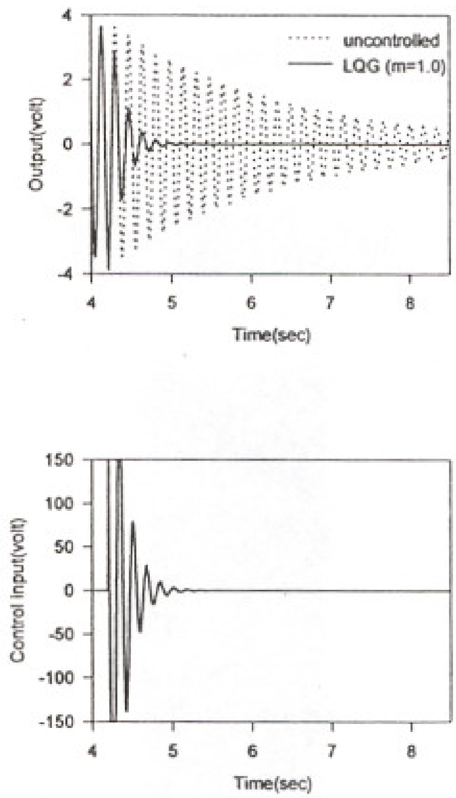

Fig. 5 Simulation results of LQ control for the first mode of beam.

Conclusions

A finite element formulations for composite structures with piezoelectric sensors and actuators has been developed. This FE procedures predicts not only modal properties but also sensing/actuating characteristics fairly well. In addition to the numerical study, the experiment for optimal vibration control of composite beams and plates has been performed. LQG control system has been designed, in which Kalman filter has been used as an observer and control gain has been determined to minimize a linear quadratic performance index. Optimal vibration control has shown the advantage in robustness to noise and in control efficiency. Also the experimental results are compared with the simulated results based on FE formulations. There has been found a good consistency between experimental and simulation results. Simultaneous control for the 1st bending and torsion modes of composite plates has been successfully accomplished using optimal vibration control method.

References

1. Bailey, T. and Hubbuard Jr. J. E., "Distributed Piezoelectric Polymer Active Vibration Control of a Cantilever Beam," *Journal of Guidance and Control*, Vol. 8, No. 5, pp. 605-611.

2. Choi, S.-B., "Alleviation of Chattering in Flexible Beam Control via Piezofilm Actuator and Sensor," *AIAA Journal*, Vol. 33, No. 3, pp. 564-567.

3. Tzou, H.S., and Gadre, M., "Active Vibration Isolation by Polymeric Piezoelectret with Variable Feedback Gains," *AIAA Journal*, Vol. 26, No. 8, pp. 1014-1017.

4. Lazarus, K.B., and Crawley, E.F. "Multivariable High-Authority Control of Plate-Like Active Structures," *AIAA SDM Conference, Paper No. 92-2529*.

5. Lee, C. K., "Theory of Laminated Piezoelectric Plates for Design of Distributed Sensors/Actuators. Part I : Govering equations and Reciprocal Relationships," *Journal of the Acoustical Society of America*, Vol. 87, No. 3, 1990, pp. 1144-1158.

6. Hwang, W. S. and Park, H. C., "Finite Element Modeling of Piezoelectric Sensors and Actuators," *AIAA Journal*, Vol 31, No. 5, 1993, pp. 930-937.

7. Reddy, J.N., *Energy and Variational Methods in Applied Mechanics*, John Wiley and Sons, Inc., New York, 1984, pp. 449-463.

Acknowledgment

This work was supported by Korea science and engineering foundation (93-0700-02-01-3). The authors are grateful to their support.

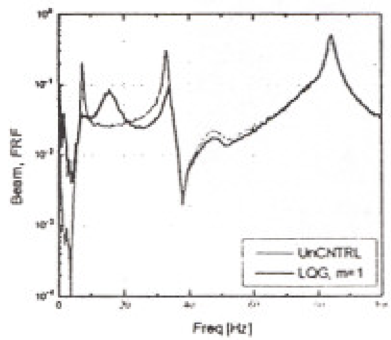

Fig. 6 FRF of controlled beam.

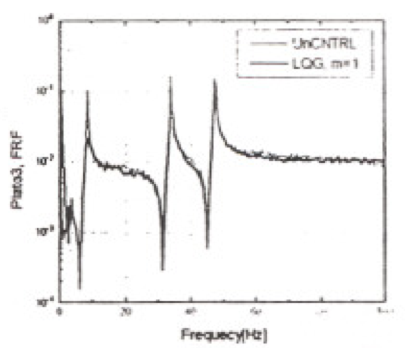

Fig. 7 FRF of controlled plate 3.

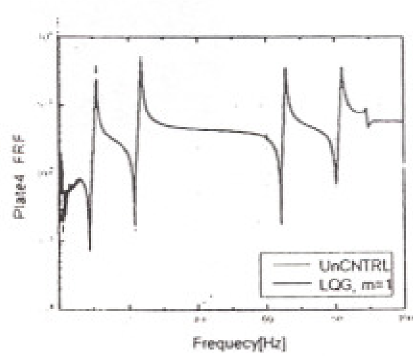

Fig. 8 FRF of controlled plate 4.